

Discontinuous Precipitation in Mg-Al Alloy Studied in 3-Dimensions

J.D Robson^{a,*}, M. J. Lawson^a, J. M. Donoghue^a, J. Guo^a, A. E. Davis^a

^a*Department of Materials, The University of Manchester, Manchester, M193PL, UK*

Abstract

Discontinuous precipitation (DP) is a commonly observed mechanism by which solid solutions decompose. It results from layers of precipitate and solute depleted matrix forming across a moving boundary. The morphology of the discontinuous regions can be highly complex, and the way dislocations or twins navigate such a structure during deformation is poorly understood. Only through 3-dimensional (3D) analysis can the true morphology of discontinuous precipitation be revealed. This work presents the first 3D study of DP using a novel PFIB based serial sectioning method. The material studied is AZ80, an industrially important class of Mg-Al alloy where DP is commonly observed. The structure is revealed to consist of an interconnected network of twisted ribbon like DP regions, which are porous and extensively branched. The width of the DP regions show strong local variations. These structures are considerably more complex than expected from classical DP precipitation theory.

Keywords: precipitation, magnesium alloys, 3D reconstruction

Discontinuous precipitation (DP) involves the the decomposition of a supersaturated solid solution into a duplex, often lamellar, transformation product consisting of precipitate and solute-depleted matrix behind a migrating grain boundary. Discontinuous precipitation occurs in over 80 binary alloy systems
5 and is of industrial interest since it generally leads to a deleterious effect on

*Corresponding author

Email address: `joseph.robson@manchester.ac.uk` (J.D Robson)

mechanical and physical properties [1, 2].

DP leads to layered structures, which can be highly complex in geometry [2], but share some morphological similarities with the layered structures formed by other mechanisms such as the eutectoid transformation [1]. In common with
10 such structures, there is usually found to be an optimum layer spacing, which corresponds to that which produces the maximum rate of free energy dissipation [3]. As DP grows outwards from a nucleation site, preserving this optimum layer spacing necessarily leads to phenomena such as layer branching [3]. In
15 a system where a preferred orientation relationship is expected between the matrix and precipitate phase, the idealized DP structure consists of unbroken parallel plates, aligned to produce the required habit plane. Such an idealized structure is rarely seen in practice [2, 3].

One good example of this is in Mg–Al alloys, the basis of the most commercially important class of AZ magnesium alloys. In this system, it is known
20 that DP does not produce favourable properties, but nonetheless it is difficult to avoid. However, the morphology of DP is usually far from the ideal picture, with both more globular and plate like regions observed, and significant deviation of the plate habit plane from an ideal crystallographic orientation [4, 5, 6]. In Mg–Al alloys, the precipitate phase is an intermetallic compound β with an
25 expected ideal composition of $\text{Mg}_{17}\text{Al}_{12}$. This phase can also precipitate via a more typical continuous mechanism of nucleation and growth of individual particles (CP). The mechanisms of CP and DP are in competition with each other, adding further complexity, and the balance of this competition is affected by supersaturation, temperature, and prior deformation [7, 8, 9].

30 One of the intriguing aspects of DP in Mg–Al alloys is the limited hardening this imparts to the alloy [10]. Even when yield is dominated by twinning, the strengthening effect associated with DP is modest. What is also surprising is that although the stress required to propagate twins in the presence of DP is increased, the twins themselves appear to cross the DP layers relatively unhindered, and retain the classic lenticular shape [11]. Since the β phase precipitates
35 are neither sheared nor twinned [12], an unbroken layer structure as expected

from the classical picture of DP would be expected to provide a very formidable obstacle to twins due to back-stresses [13]. This is not observed in practice, leading to the previously unproven suggestion that in 3D there is a pathway for
40 twins to bypass precipitate layers that in 2D appear as continuous obstacles.

A key obstacle to understanding the complex DP morphologies observed in Mg-Al and how they influence phenomena such as twin propagation is that all current microstructural information comes from 2D sections. This limitation is particularly acute when considering layered and branched structures,
45 where the direction of sectioning can give a completely different impression of the microstructure. This was recognised over a century ago in the analysis of the pearlite structure, a eutectoid transformation product with morphological similarities to DP [14]. Pioneering work involving serial sectioning and optical microscopy was used to reconstruct the true 3D nature of pearlite, and provided
50 important insights to help explain its structure and mechanism of formation.

The tools available for 3D analysis of microstructures are now much more advanced, but the principle of reconstructing the 3D structure from a stack of 2D slices remains unchanged [15]. In the present work, a state-of-the-art serial sectioning study was undertaken to reconstruct the 3D structure of DP
55 in a commercial Mg-Al-(Zn) alloy (AZ80). To the authors knowledge, this is the first 3D analysis of DP, and provides new insights to help understand both the mechanism of formation and the poor strengthening effect produced by DP structures.

The material used is a commercial AZ80 alloy (nominal composition range
60 7.8-9.2 Al 0.2-0.8 Zn 0.12-0.5 Mn wt%, balance Mg), provided as direct chill cast ingot by Luxfer MEL Technologies, Manchester, UK. The as cast material was homogenised at 400°C for 24 h using an argon gas furnace, and then hot rolled on a laboratory mill at 400°C to a total reduction of 80%. This material was then solution treated for 1 h at 420°C, leading to the desired equiaxed grain
65 structure with a basal texture and supersaturated solid solution. Precipitation heat treatment was carried out for 16 h at 220°C. This temperature was chosen since it corresponds to a condition where DP is expected to dominate [7], en-

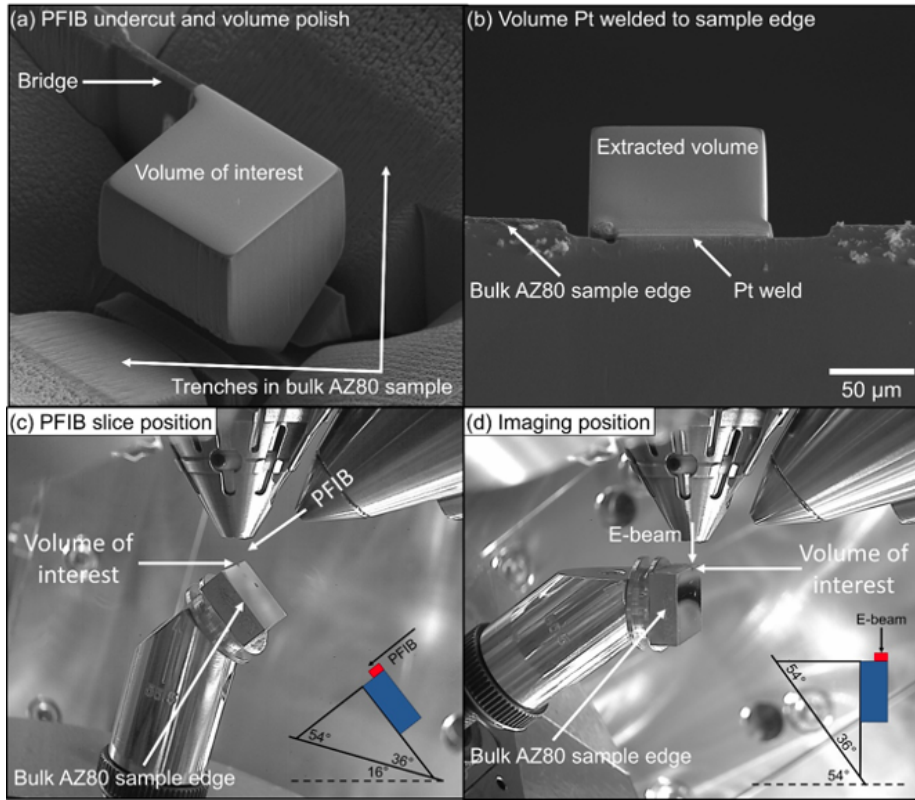


Figure 1: (a) shows the extraction trenches around the Pt-coated volume of interest that is still attached via the bridge, (b) shows the volume Pt-welded to the sample edge, ready for slicing and imaging. (c-d) PFIB in-chamber views with inset (exaggerated) schematic showing the (c) PFIB serial slicing position and (d) imaging position.

abling the morphology of the DP to be studied without the complicating effect of CP.

70 A Thermo Scientific Helios 5 PFIB system was used to extract the volume of
 interest from the sample bulk and prepare it for 3D slicing and imaging. Before
 extracting the $\approx 100 \times 100 \times 100 \mu\text{m}$ volume, the top surface was protected
 by a platinum (Pt) coating deposited using a gas injection system in the PFIB
 operated at 12 kV and 50 nA. Four $\approx 150 \times 100 \mu\text{m}$ trenches were then dug
 75 around the sample with a 30 kV accelerating voltage and a $1 \mu\text{A}$ current, where
 each trench extended beyond the volume of interest to allow redeposited material

to escape during the subsequent undercuts. A $10\ \mu\text{m}$ bridge was left to keep the volume of interest attached to the sample bulk for the undercuts. Fig. 1(a) shows the volume-bridge-sample layout after undercutting. The volume edges were ‘cleaned’ with the PFIB at this stage to remove redeposited material and polish the exposed side faces with a probe current of 60 nA. A novel method for mounting the volume for serial slicing was used where the volume was mounted back onto the bulk material it was lifted out from, which meant that at no point did the system need to be vented during the process.

The volume of interest was extracted using a micromanipulator (after severing the bridge) and then attached directly to the edge of the sample using i-beam deposited platinum, as shown in Fig. 1(b), so that the volume protruded from the sample side edge. The sample was mounted to a 36° pre-tilted holder so that the surface for examination was tilted to 54° relative to the stage. For PFIB slicing (Fig. 1(c)), the stage was tilted to 16° so that the examined surface was parallel to the PFIB (52°), and a 30 kV accelerating voltage and 60 nA current was used to remove $\simeq 100\ \text{nm}$ of material per slice, which was assisted by fiducial tracking to maintain slicing-resolution accuracy. In addition, to prevent the development of PFIB-induced curtains, a rocking mill was employed so that the sample was sliced at alternating $+$ and -5° angles.

For imaging (Fig. 1(d)), the stage was tilted to 54° , so that the surface was perpendicular to the electron beam (90°), and images were collected every 2 slices (every 200 nm for the same rocking mill angle) using the through-the-lens detector in BSE mode with an 8 kV accelerating voltage, 26 nA current, and a 4 mm working distance. Overall, 500 images were collected throughout the $100\ \mu\text{m}$ -thick volume, which were then processed and reconstructed into a 3D image.

The raw SEM images were filtered (FFT filter) to remove the curtain artefacts from the FiB process. They were then batch binarised in ImageJ [16] so that the Mg matrix and continuous precipitation could be removed leaving only the DP. The 3D image stack was then imported to Avizo (v2020.2, Thermo Scientific) where the image stack was aligned, to correct for drift during acquisition,

using the ‘Align Slices’ module. This was achieved semi-automatically using the edge detection algorithms combined with manual definition of the edges of the cut surface. Once the 3D image stack was aligned a label analysis was performed
110 to measure the characteristics of each individual area of DP. These results were also visualised as volume renderings in Avizo. A version of the full 3D dataset was also exported in a format suitable for rendering in the open source software Paraview to allow the interested reader to inspect the 3D data for themselves.

115 Figure 2 shows SEM images of the microstructure revealing that, as intended, the grains have been fully invaded by DP. The complex morphology is revealed, with more globular and more plate-like regions apparent. The DP does not appear as unbroken layers, as expected from the simple classical picture, but instead forms as apparently isolated particles. DP regions can also be seen to
120 bend, and are not obviously confined to grow along a well defined habit plane.

In such 2D sections the true nature of the DP structure is hidden and important questions remain unanswered. For example, are the different morphologies observed truly different, or is this an artefact of sectioning? Are the DP regions that appear as isolated particles actually part of a continuous layer that con-
125 tinues sub-surface? Finally, are the DP regions with different alignment within one grain related/interconnected, or are they due to different nucleation events? Such questions can be addressed only with a 3D evaluation of the microstructure.

An isometric projection of the full 3D volume is shown in Figure 3. Since
130 it is difficult to present 3D data in 2D, the reader is invited to inspect the full 3D dataset for themselves. The 3D dataset shows the precipitates apparently radiating from a single point or line. The precipitate plates are not continuous layers in any plane, but rather are broken by gaps and holes in the structure. Often the plates can deviate markedly from a single habit plane.

135 The morphology of DP in the Mg-Al system was previously described on the basis of transmission electron microscopy (TEM) analysis as twisting ribbons [4]. The 3D dataset fits well this description and shows that even when a plate appears to be straight when viewed in one section, it is actually bent and

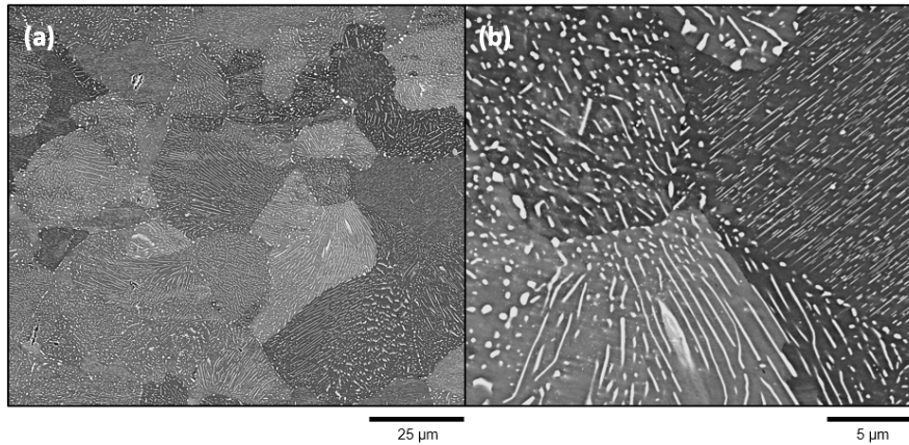


Figure 2: Backscattered SEM images taken independently from the serial-sectioning study on an SEM (5 kV, 0.8 nA) equipped with a high-sensitivity backscattered electron detector showing (a) low magnification showing total invasion of discontinuous precipitation (DP). (b) Higher magnification showing details of the plate morphology as seen in 2D

twisted when viewed in other planes. Note that the steps that appear in the
 140 3D reconstruction are artefacts of the serial sectioning method rather than real
 features of the microstructure. No attempt was made to smooth these steps,
 since this can potentially introduce artificial features in the reconstruction.

To facilitate visualization, a subset of the data presented in Figure 3 is shown
 in Figure 4. In this case, the commercial software package Avizo (v2020.2,) was
 145 used to perform the image rendering and analysis. In Figure 4(a), features
 that are interconnected are assigned the same colour. Therefore, all of the DP
 plates coloured blue are actually interconnected and form one large structure.
 Indeed, it is possible that even the small regions that are assigned different
 colours are also part of the same structure, but due to the cropping effect the
 150 connection points lie outside the analysed region. This confirms that what
 appear as individual particles in a 2D (e.g. Figure 4(b)) are actually branches
 of a single, large, colony structure. This is consistent with the understanding
 that a DP colony can form from a single nucleation site, then grow and branch

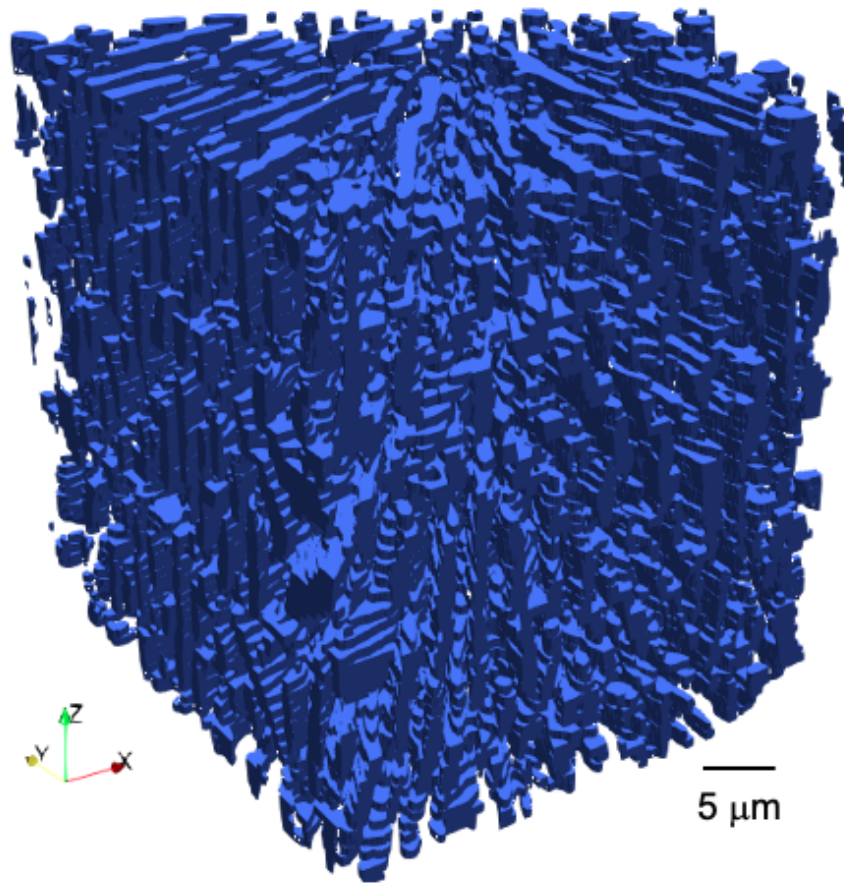


Figure 3: Near isometric projection of full 3D dataset showing DP regions (blue), visualized using Paraview.

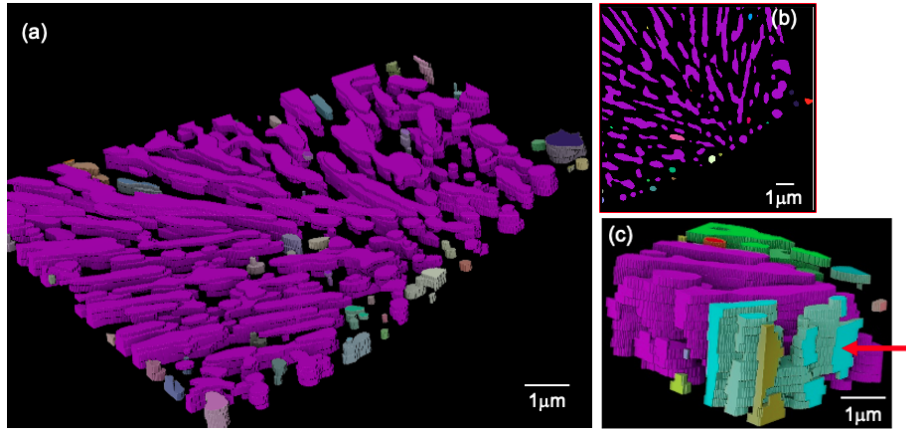


Figure 4: (a) Selection of 3D dataset visualized in Avizo; features in the same colour are interconnected. (b) Section demonstrating that interconnection of features in the same colour is not apparent in 2D. (c) Zoomed in region showing an example of plate branching (arrowed).

until it invades an entire grain [2]. Figure 4(c) is a further zoomed in region, showing branching, as illustrated by the DP region coloured cyan and identified by an arrow. Looking from the bottom of this image towards the top, it can be seen that this plate splits, leaving a gap between the two branches. Such splitting/branching is very commonly observed.

Several useful parameters can be quantified from the 3D dataset using the analysis tools available in Avizo. The overall volume fraction of DP was determined to be $28 \pm 5\%$. This is significantly higher than the maximum theoretical volume fraction of 13%, as calculated using thermodynamic modelling software (JMatPro version 12.4 with the magnesium database). Given the aging treatment was chosen to be sufficiently long to produce a fully DP microstructure, the true volume fraction is expected to be close to this maximum value. The significant over-estimate from the measurement of the 3D dataset is a common problem when thresholding from SEM images. For example, analysis of the data confirmed that blurring around the precipitates (caused by the relatively high accelerating voltage electron beam interacting with non-parallel plate volumes below the sample surface) is often incorrectly segmented during thresholding.

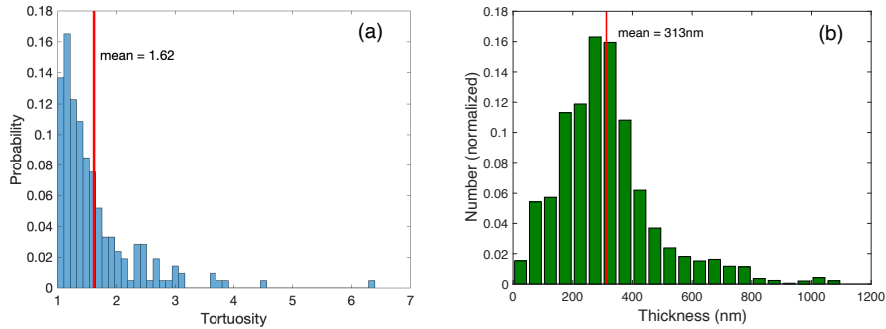


Figure 5: (a) Histogram of measured tortuosity (b) Histogram of maximum plate thickness (determined by maximum diameter of a sphere that can be wholly contained within the plate).

This will lead to an over-estimate in the absolute measurement of layer thickness, but it does not affect the important observations about the structure and morphology of the DP, which is the focus of this paper.

The tortuosity of the layers as calculated by Avizo [17] is plotted in Figure 5(a). The tortuosity describes how straight the layers are (a value of 1 corresponds to a perfectly straight layer). It can be seen there is a wide distribution of values, reflecting the observation that some layers are very bent or twisted whereas others are quite straight.

The thickness distribution of the β layers is shown in Figure 5(b). Note that the thickness is calculated by determining the diameter of the largest sphere that can fit inside the layer object [18]. It is notable that there is a very wide variation in the measured thickness. In the idealized theoretical model of DP growth, the layer thickness is constant and controlled by a balance between surface energy and diffusional processes [19]. It can be seen that over the large volume studied here, the layer thickness is far from this idealized picture. Previous studies using TEM to measure layer thickness values give much smaller values of the layer thickness, of around 30 nm [4]. However, as demonstrated here, strong local variations are possible, both within grains and between them. Neither TEM, nor even the much larger volume studied here, is likely to be sufficient to obtain a statistically reliable layer spacing measurement for the entire microstructure.

In summary, this paper presents what is (to the authors knowledge) the first 3D study of discontinuous precipitation (DP) in an alloy system. Using a PFIB and a novel specimen mounting process has enabled a relatively large volume to be sectioned at sufficient resolution to capture the details of the DP in 3D
195 with high image quality. DP is proved to consist of an interconnected network of plates forming a precipitate crystal that is interwoven with the matrix. It has been demonstrated that the plates are ribbon-like and often bent, twisted, and branched. This structure results in large gaps between the plates in all directions, and this is likely to explain why such plates do not strongly prevent
200 the growth of twins or effectively block gliding dislocations.

Acknowledgements: Luxfer MEL are thanked for the provision of materials for this research. The EPSRC are thanked for financial support via LightFORM (EP/R001715/1). JDR acknowledges the DSTL/RAEng Chair in Alloys for Extreme Environments. The authors acknowledge the use of equipment associ-
205 ated with the Advanced Metals Processing and Characterisation themes of the Henry Royce Institute for Advanced Materials, funded through EPSRC grants EP/R00661X/1, EP/S019367/ 1, EP/P025021/1 and EP/P025498/1. The data required to reproduce these findings are available from the LightFORM Zenodo repository <https://doi.org/10.5281/zenodo.7108545>.

210 1. References

References

- [1] J. W. Christian, *The Theory of Transformations in Metals and Alloys*, Elsevier, 2002.
- [2] D. B. Williams, E. P. Butler, Grain boundary discontinuous precipitation
215 reactions, *International Metals Reviews* 26 (1) (1981) 153–183.
- [3] I. Manna, S. Pabi, W. Gust, Discontinuous reactions in solids, *International Materials Reviews* 46 (2) (2001) 53–91.

- 220 [4] D. A. Porter, J. W. Edington, Microanalysis and cell boundary velocity measurements for the cellular reaction in a Mg-9% Al alloy, *Proceedings of the Royal Society A: Mathematical, Physical and Engineering Sciences* 358 (1694) (1978) 335–350.
- [5] D. Duly, M. C. Cheynet, Y. Brechet, Morphology and chemical nanoanalysis of discontinuous precipitation in Mg-Al alloys—I. regular growth, *Acta Metall. Mater.* 42 (1994) 3843–3854.
- 225 [6] D. Duly, M. C. Cheynet, Y. Brechet, Morphology and chemical nanoanalysis of discontinuous precipitation in Mg Al alloys II. irregular growth, *Acta metallurgica et materialia* 42 (11) (1994) 3855–3863.
- [7] D. Duly, S. Simon, B. Brechet, On the competition between continuous and discontinuous precipitations in binary Mg-Al alloys, *Acta Metallurgica et*
230 *Materialia* 43 (1) (1995) 101 – 106.
- [8] J. Robson, Modeling competitive continuous and discontinuous precipitation, *Acta Materialia* 61 (20) (2013) 7781–7790.
- [9] J. Robson, J. Guo, A. Davis, Modelling the effect of deformation on discontinuous precipitation in magnesium—aluminium alloy, *Alloys* 1 (2022)
235 54–69.
- [10] D. Duly, Y. Brechet, B. Chenal, Macroscopic kinetics of discontinuous precipitation in a Mg-8.5 wt% Al alloy, *Acta metallurgica et materialia* 40 (9) (1992) 2289–2300.
- [11] N. Stanford, A. Taylor, P. Cizek, F. Siska, M. Ramajayam, M. Barnett,
240 *Twinning in magnesium-based lamellar microstructures*, *Scripta Materialia* 67 (7-8) (2012) 704–707.
- [12] N. Stanford, J. Geng, Y. B. Chun, C. H. J. Davies, J. F. Nie, M. R. Barnett, Effect of plate-shaped particle distributions on the deformation behaviour of magnesium alloy AZ91 in tension and compression, *Acta Ma-*
245 *terialia* 60 (1) (2012) 218–228.

- [13] J. D. Robson, The effect of internal stresses due to precipitates on twin growth in magnesium, *Acta Materialia* 121 (2016) 277–287.
- [14] M. D. Graef, M. Kral, M. Hillert, A modern 3D view of an “old” pearlite colony, *JOM* (2006).
- 250 [15] P. G. Kotula, G. S. Rohrer, M. P. Marsh, Focused ion beam and scanning electron microscopy for 3D materials characterization, *MRS Bulletin* 39 (4) (2014) 361–365.
- [16] C. A. Schneider, W. S. Rasband, K. W. Eliceiri, NIH image to ImageJ: 25 years of image analysis, *Nature methods* 9 (7) (2012) 671–675.
- 255 [17] R. Harwood, G. Th eroux-Rancourt, M. Barbour, Understanding airspace in leaves: 3D anatomy and directional tortuosity., *Plant Cell Environ* 44 (8) (2021) 2455–2465.
- [18] R. Dougherty, K.-H. Kunzelmann, Computing local thickness of 3D structures with ImageJ, *Microscopy and Microanalysis* 13 (S02) (2007).
- 260 [19] L. M. Klinger, Y. J. M. Brechet, G. R. Purdy, On velocity and spacing selection in discontinuous precipitation–I. simplified analytical approach, *Acta Materialia* 45 (12) (1997) 5005 – 5013.